Reviews

Scintillator Materials

G. Blasse

Debye Institute, University of Utrecht, Postbox 80.000, 3508 TA Utrecht, The Netherlands

Received March 29, 1994. Revised Manuscript Received May 26, 1994[⊗]

Scintillators are materials which can detect highly ionizing radiation, because they efficiently convert the energy of this radiation into light. After defining this field of materials, the physical phenomena in scintillators are briefly discussed. Many applications of scintillators are known, and the more important ones are dealt with. From this discussion the requirements which scintillator materials have to satisfy are derived. The materials which are of importance at the moment, or have potential for the future are discussed. Finally some problems for the near future are commented upon.

1. Introduction

Not only X-rays but also α-, β-, and γ-rays were discovered because they are able to excite phosphors such as $K_2Pt(CN)_4$ (1895 by Röntgen and 1896 by Becquerel, respectively). To detect these rays, photographic plates have a large disadvantage, because they hardly absorb the radiation concerned. Therefore, other detection methods have been looked for. Scintillators are luminescent materials which absorb this type of radiation efficiently and convert the absorbed radiation into radiation with a wavelength in or around the visible spectral region. The emitted radiation is detected by a photomultiplyer or a photodiode. These instruments convert the visible radiation into an electric signal.

By way of illustration, we mention here three scintillators which have found application: (i) $CaWO_4$, which was already used in 1896 to convert X-rays into blue light and made X-ray photography of the human body possible; it was used for some 75 years as an X-ray phosphor (powder screens). (ii) $NaI:Tl^+$, which is in use for some decades as an γ-ray detector. Large single crystals are used in γ cameras. (iii) $Bi_4Ge_3O_{12}$ (BGO), found as an X-ray phosphor by Weber (1973), but also able to detect other types of radiation. It is nowadays used in crystalline form in positron emission tomography (a medical-diagnostic method to be discussed below and based on γ-ray detection) and in the largest electromagnetic-radiation calorimeter in the world (CERN, Geneva, since 1989), which consists of 12 000 $Bi_4Ge_3O_{12}$ crystals of 24 cm in length with a total volume of 1.2 m^3. This calorimeter is able to measure precisely the energy of electrons, positrons, and photons produced in energetic collisions in a collider.

These examples illustrate also that the range of applications of these materials is very wide. In recent years the interest in scintillators revived, partly because it was realized that the understanding of luminescent processes in other materials had progressed considerably, partly because a new type of scintillation, known as cross luminescence, was detected and partly because many applications require materials with improved properties. This situation is well described in a recent workshop report.[1]

In this paper the state-of-the-art is reviewed with emphasis on the scintillator materials. In section 2 the physics of scintillators, which is far from understood, is discussed. In section 3 the possible applications of scintillators are shortly reviewed, without aiming for completeness. In section 4 we will discuss the scintillator materials. First we derive the requirements which they have to satisfy in order to be of interest for applications. Subsequently a number of specific materials in use at present are dealt with, together with some recently proposed new materials. A look into the future comprising predictions on the type of research needed closes the review.

For many elaborate treatments of a general nature we refer to the literature.[1-5]

2. Physical Phenomena in Scintillators

It is useful to divide the overall scintillation process into three parts, viz.,[2,3,6] (i) the conversion process in which the energy of the incoming radiation or particles is converted into a large number of electron−hole pairs, (ii) the transfer process in which the energy of an electron−hole pair is transferred to the luminescent ion involved, and (iii) the emission process in which the luminescent ion returns radiatively from an excited state to the ground state.

The energy efficiency η of a scintillator can then be written as

$$\eta = \gamma S q \qquad (1)$$

[⊗] Abstract published in *Advance ACS Abstracts,* July 1, 1994.

(1) De Notaristefani, F., Lecoq, P., Schneegans, M., Eds.; *Heavy Scintillators for Scientific and Industrial Applications*; Editions Frontières: Gif-sur-Yvette, France, 1993.

(2) Blasse, G.; Grabmaier, B. C. *Luminescent Materials*; Springer-Verlag: Berlin, 1994.

(3) Lempicki, A.; Wojtowicz, A. J.; Berman, E. *Nucl. Instrum. Methods* **1993**, *A333*, 304; *J. Lumin.* **1994**, *60/61*, 942.

(4) van Eijk, C. W. E. *Nucl. Tracks Radiat. Meas.* **1993**, *21*, 5; *J. Lumin.*, in press.

(5) Schotanus, P. *Nucl. Tracks Radiat. Meas.* **1993**, *21*, 19.

(6) Robbins, D. J. *J. Electrochem. Soc.* **1980**, *127*, 2694.

0897-4756/94/2806-1465$04.50/0

Here γ and S are the efficiencies of the conversion and the transfer processes, respectively. Further, q denotes the quantum efficiency of the luminescent center.

It is important to realize that the energy E which is necessary to create the average electron–hole pair is much larger than that of the pair, i.e., $E = \beta E_g$ ($\beta > 1$). Shockley estimated that $3E_g$ is needed per pair, where E_g is the bandgap energy.[7] Later, Robbins showed that this value can vary between $2.3E_g$ and $7E_g$, depending on the host lattice.[6] The higher values are found for the lattices with higher vibrational frequencies (e.g., $CaWO_4$, YVO_4). In addition the emitted radiation generally will be situated at energies below E_g. Therefore $\gamma = (E_{em}E_g^{-1})(E_gE^{-1})$, where E_{em} is the energy of the emission maximum. This implies that a scintillator with $E_g = 5$ eV, blue emission ($E_{em} = 3$ eV), and a β value of 3, has $\gamma = 0.2$, so that 80% of the absorbed energy is already lost for the luminescent emission. For a given host lattice it is possible to estimate the value of β, so that the value of γ can also be estimated, since the values of E_g and E_{em} can be easily obtained spectroscopically. It is important to realize that this procedure teaches us in a simple way whether a given compound will be an efficient scintillator lattice or not (see Table 1). The procedure is reasonably reliable.[8]

This is no proof that the conversion process is understood. The Shockley–Robbins approach is generally used in the Western world, but peculiarly enough the Eastern-European world follows a different model[9] in which fast electrons lose energy primarily to plasmons.[10] Since this yields also β values of the order 3, the materials scientist will not worry too much: although the physical processes are not yet understood, there are methods available to estimate the conversion efficiency of a potential scintillator material.

Now that the electron–hole pairs have been formed with a certain efficiency, we return to eq 1 and wonder what can be said about S and q.

The transfer efficiency S is 1 only if the electron–hole pair is exclusively captured by the luminescent center. As soon as the pair ends its life in a different way, the value of S becomes smaller than 1. It is well-known that solids offer many possibilities for an electron–hole pair to end its life somewhere else. As an example we mention radiative and nonradiative electron–hole pair recombination and capture by defects and impurities which results in an undesirable or often no emission at all.

The prescription to obtain a material with S close to 1 is obvious, although vague. First, the luminescent ion itself should show a strong preference to capture either a hole or an electron. Second, the host lattice should be as perfect as possible. The latter statement excludes solids with a complicated or doubtful composition, and amorphous materials for use as efficient scintillators. The optimization of S is a challenging task for the solid-state or materials chemist.

The quantum efficiency of the luminescent center can be determined directly by exciting the center with ultraviolet radiation (photoluminescence). Nowadays there exists also a reasonable understanding of the factors which determine the value of q, which makes an estimation possible.[2] Many luminescent centers with q close to 1 are known. The unpredictable character of η (eq 1) lies therefore in the transfer efficiency S.[3,8]

Table 1. Some Data on Compounds Which Are or Might Be Good Scintillators (from Refs 3 and 6)[a]

compound	$\hbar\omega$ (eV)	E_g (eV)	β
CsI	0.011	6.4	2.5
NaI	0.022	5.9	2.7
ZnS	0.044	3.8	2.9
$Bi_4Ge_3O_{12}$	0.045	5.0	3.3
CeF_3	0.057	10.4	3.8
La_2O_2S	0.057	4.4	4.0
Y_2O_3	0.068	5.6	4.6
$LuPO_4$	0.133	8.7	6.1
$CaWO_4$	0.112	4.6	7
YVO_4	0.116	3.7	7.5
CeP_5O_{14}	0.161	8.7	7.8

[a] $\hbar\omega$: optical phonon energy. E_g: bandgap energy. β: EE_g^{-1}, calculated according to ref 6.

It should be remarked that eq 1 relates to that part of the exciting radiation that is absorbed by the scintillator. Therefore the more general expression is

$$\eta = (1 - r)\gamma Sq \qquad (2)$$

where r is the amount of radiation that is not absorbed but either reflected or transmitted. The value of r can be minimized by the materials choice. Generally speaking, scintillators are compounds of heavy elements with high density. For X-ray and γ-ray excitation, for example, this is essential. But for neutrons, specific elements are required (B, Li, Gd).

3. Applications of Scintillators

Scintillators are usually applied as large crystals. The applications are found in medical diagnostics, in industry, and in science.[1] Their number is large, so we will restrict ourselves to representative examples. The most spectacular application is the use of scintillators in electromagnetic calorimeters: the largest was built at CERN (Geneva) in the late eighties and contains 12 000 $Bi_4Ge_3O_{12}$ crystals of 24 cm in length, representing a total volume of 1.2 m^3.[11] Plans exist to build a new generation of high-precision calorimeters which need an even larger amount of crystals (60 m^3 CeF_3). However, the cost seems to limit this development. These calorimeters are used in high-energy physics, nuclear physics, and astrophysics to count electrons and photons.

The energy of the radiation or of the particles involved is usually very high and may range up to the gigaelectronvolt area. As a consequence, the conversion efficiency of the scintillator can be low. A light yield of only ~200 photons/MeV suffices. The reader should note that for emitted photons of about 4 eV this corresponds to an energy efficiency of only 0.08%. It is exceptional in the field of luminescence that such a low efficiency suffices for an application.

However, in almost all other cases a high light yield is important. The accuracy of the observation is higher if the number of observed photon, N, is larger. Energy

---

(7) Shockley, W. *Czech. J. Phys.* **1961**, *11*, 81.
(8) Blasse, G. *J. Lumin.* **1994**, *60/61*, 930.
(9) Rodnyi, P. A., private communication.
(10) Rothwarf, A. *J. Appl. Phys.* **1973**, *44*, 752.
(11) Lecoq, P., *J. Lumin.* **1994**, *60/61*, 948.

and time resolution are proportional to $1/\sqrt{N}$. The basic principle of scintillation counting is that the light output of the scintillator is proportional to the energy of the incident photon.[12] To detect these photons, the scintillator is coupled to a photomultiplier tube in which the photons are converted into photoelectrons which are multiplied and give a pulse with an amplitude proportional to the number of photons. For a linear detector response all components should also have a linear response.

A γ-ray spectrometer should be able to discriminate between γ-rays with slightly different energy. This quality is characterized by the so-called energy resolution which depends on the light yield as indicated above.

The time resolution is defined as the ability to give accurately the moment of absorption of the photon in the scintillator. The time resolution is proportional to $1/\sqrt{N}$ and the decay time τ. It is obvious that the moment of the absorption event is found most accurately if τ is short.

Scintillators also play an important role in medical diagnostics. First, we mention the γ-ray camera. Radioisotopes are injected into the body, usually in the form of chemical compounds labeled with a suitable radioactive element. A commonly used one is ^{99m}Tc. By measurement of the radiation outside the body, a functional image can be obtained. The emitted radiation (120−150 keV) is measured by a γ-ray camera which usually contains a scintillator crystal. Common γ-ray cameras yield a two-dimensional image of the radioactivity distribution. When the camera is rotated around the patient and/or two opposed γ-ray cameras are used, it is possible to construct a three-dimensional image. This technique is called SPECT (single-photon emission computed tomography). This method does not allow to make accurate corrections for radiation attenuation in the body. Therefore, SPECT does not produce very good images, especially not of deeper-lying organs.

A different method is PET (positron emission tomography). It is also an in vivo tracer technique but uses the annihilation of positrons. Actually one is confined to positron emitters for in vivo studies of the distribution of elements in biologically active compounds, such as carbon, nitrogen, and oxygen. Metabolic processes can be studied in this way.

The emitted positron cannot penetrate far in tissue; its range is only a few millimeters. After slowing down, it annihilates with an electron. In most cases two photons (γ-radiation) are emitted with an electron of 511 keV each under 180°. PET exploits the collinear emission by putting a coincidence requirement on detectors opposed to each other: an event detected simultaneously in the two detectors implies that the annihilation took place somewhere along the line between the two points of detection (Figure 1). From the coincidence data, images are constructed which present the three-dimensional distribution of the radioactivity. The images are corrected for radiation attenuation in the body which is not possible with SPECT.

As mentioned above, the scintillation light can be detected using a photomultiplyer. There are also other possibilities. Among the solid-state photon detectors, the silicon photodiodes have become popular. Their sensitivity reaches a maximum for wavelengths longer than 500 nm.

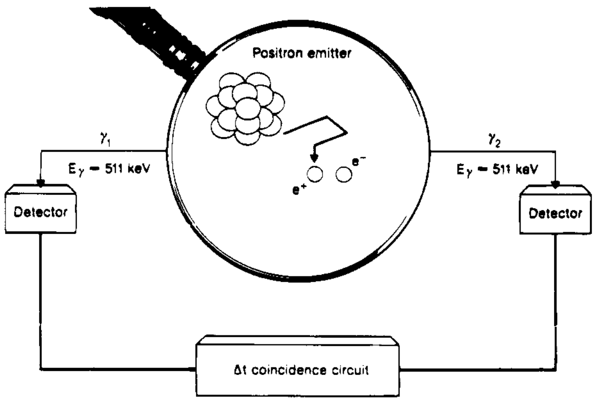

Figure 1. Principle of positron emission tomography. Behind the magnifying glass the positron (e$^+$) emission is shown. Its annihilation with an electron (e$^-$) yields two γ-quanta under an angle of 180°. After Grabmaier, p 70 in ref 1.

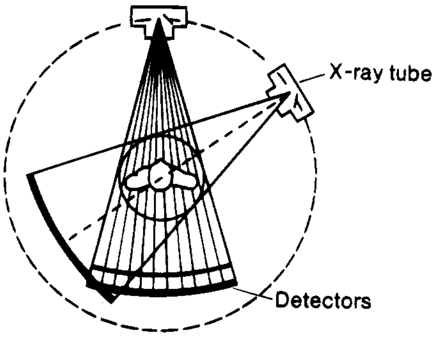

Figure 2. Principle of computed tomography (see also text). The fixed system of X-ray tube and detectors rotate around the patient.

A different detection unit is the solid-scintillator proportional counter.[13] It consists of a scintillator with ultraviolet emission in a multiwire chamber filled with an organic vapor. The organic molecules are ionized by the ultraviolet photons and the resulting photoelectrons are detected in the multiwire chamber. A popular molecule for this application is TMAE (tetrakis(dimethylamino)ethylene).

Industrial applications form a very broad field in which imaging as well as counting techniques are applied. We mention X-ray tomography, oil well logging, process control, security systems, container inspection, mineral processing, and coal analysis.[1]

The detection of X-rays by luminescent materials was discussed in an earlier review which also mentioned the storage phosphors.[14] In the present context the computed tomography should be mentioned. The principle is based on the detection of a series of X-ray attenuation profiles from several different viewing directions, which subsequently allow the reconstruction of cross sectional images of an object. From a variety of technical systems for CT machines the so-called fan-beam design has proven to be the most advantageous. In Figure 2 a CT scanning system following the rotation−rotation principle is illustrated. In such a system, the X-ray tube and detector are rigidly coupled and rotate around the measurement field within a few seconds. A fan-shaped

---

(12) Knoll, G. F. *Radiation Detection and Measurement*, 2nd ed.; Wiley: New York, 1989.

(13) Anderson, D. F. *Phys. Lett.* **1982**, *B118*, 230.

(14) Blasse, G. *Chem. Mater.* **1989**, *1*, 294.

Table 2. Scintillator Requirements in Various Applications (after Ref 17)

application	light yield (photons/MeV)	decay time (ns)	emission (nm)
Counting Techniques			
calorimeter (high-energy physics)	>200	<20	>450
calorimeter (low-energy physics, nuclear physics)	high	varies	>300
positron emission tomography (PET)	high	<1	>300[a]
γ-ray camera	high	less imperative	>300
industrial applications	high	varies	>300
Integrating Techniques			
computed tomography (CT)	high	no afterglow	>500
X-ray imaging	high	less imperative	>350

[a] But <250 nm when using a multiwire chamber.

beam of X-rays continuously passes through a cross-sectional "slice" of the patient and hits the detector system. To be able to reconstruct CT images, attenuation profiles (projections) of that part of the patient's body located in the measurement field are scanned from several different viewing directions. The attenuation profiles are registered in a "single shot" for each viewing direction as an X-ray intensity pattern by means of a linear detector array system.

Modern CT scanners use detector arrays with at least 1000 individual X-ray detecting channels. Each detector element is about 1 mm wide. The spacing between the elements is rather small but is present to suppress cross talk by interstitials, to minimize the loss of dose utilization.

For solid-state detectors the phosphor–photodiode concept is preferred. The X-rays absorbed by the phosphor are converted into visible radiation, which propagates to the photodiode coupled to the phosphor element at the side opposite to the incident X-ray. Then, an electrical signal is generated by the photoelectric conversion of visible light.

Finally we mention the possibilities of particle identification by using a scintillator crystal. This method makes use of the fact that certain scintillators, for example BaF_2, $CsI:Tl^+$ and organic materials, show two different emissions, one with a shorter and one with a longer decay time (see also below). Wisshak et al. were able to discriminate γ-photons and charged hadrons using a BaF_2 scintillator.[15] A more general example, also using BaF_2, has been given by Migneco et al.[16]

The intensity ratio of the fast and the slow emissions depends on the nature of the particle. The contribution of the fast component decreases in the sequence γ-rays and cosmic muons, protons, deuterons, tritons, and α particles. The penetration depth decreases in the same sequence, i.e, the excitation density increases. This will be discussed further in the sections on organic scintillators (section 4.2) and on BaF_2 (section 4.3).

4. The Materials

4.1. Requirements. Table 2 gives a survey of the scintillator requirements in the various applications according to an idea by Van Eijk.[17] Integrating techniques are used when high counting rates exclude the use of counting techniques. As a matter of fact the atomic number of the constituents as well as the density should be high. An exception to this are scintillators for neutron detection; they should contain Li, B, or Gd. Further, scintillator materials should be rugged and radiation hard. Of course they should not be hygroscopic. The emission range is a.o. dictated by the detector used. The light yield should be high; only in the large calorimeters used in high-energy physics in the large colliders this requirement is not important.

In section 2 it was discussed how the efficiency can be estimated for a given composition. As a matter of fact the quantum efficiency of the luminescent center should be high, and competing (quenching) centers should be absent. Let us consider a well-known scintillator, such as $NaI:Tl^+$, by way of illustration. The literature reports for this scintillator a light yield of 40 000 photons/MeV (ph/MeV). Since the emission band of $NaI:Tl^+$ peaks at about 3 eV, the energy efficiency η amounts to 12%.[8] The procedure according to Robbins predicts a maximum efficiency of 19%. This indicates that either S or q (eq 1) or both have a value <1.

Short decay times can be obtained by using luminescent ions with allowed emission transitions. In the field of inorganic materials the best examples are the $5d \rightarrow 4f$ transitions ($\tau \sim 10$ ns) and the cross-luminescence ($\tau \sim 1$ ns). The afterglow is governed by the presence of traps in the host lattice. We will now consider several scintillator materials which are in use or which have a potential for applications.

4.2. Organic Scintillators. Organic scintillators, often used as plastics, have as large advantages the ease of fabrication, low cost, and short decay times ($\sim$1 ns). Due to their low density ($\sim$1 g cm^{-3}) they are not suitable for γ- and X-ray detection. However, for the detection of charged particles they may be suitable.[12]

Organic scintillators can also be used for particle discrimination. Apart from the fast (and dominating) luminescence component (fluorescence), there is also a slow component (delayed fluorescence). The fraction of the luminescence appearing in the slow component depends often on the nature of the exciting particle. Therefore, the intensity ratio of the slow and the fast components contains information on the nature of the exciting particles.

The delayed fluorescence is due to the fact that long-lived triplet states of organic molecules meet and annihilate each other, so that a singlet state is formed which yields fluorescence.[12] The probability for such bimolecular interactions increases if the excitation density is higher. Particles with a low penetration depth yield a higher excitation density and therefore a stronger slow component. For example, the slow component has an increasing intensity in the sequence γ-rays, neutrons, and α-particles.[12]

4.3. BaF_2 and Cross-Luminescence. The compound BaF_2 shows two different emissions. Their origin and properties are strikingly different. Excitation with energies above 10 eV (the bandgap energy) yields an emission around 300 nm with a decay time of 600 ns at room temperature. This emission is due to anion

---

(15) Wisshak, K.; Guber, K.; Käppeler, F.; Krisch, J.; Müller, H.; Rupp, G.; Voss, F. *Nucl. Instrum. Methods* **1990**, *A292*, 595.

(16) Migneco, E.; Agodi, C.; Alba, R.; Bellin, G.; Coniglione, R.; Del Zoppo, A.; Finocchiaro, P.; Maiolino, C.; Piattelli; Raia, G.; Sapienza, P. *Nucl. Instrum. Methods* **1992**, *A314*, 31.

(17) van Eijk, C. W. E., p 601 in ref 1.

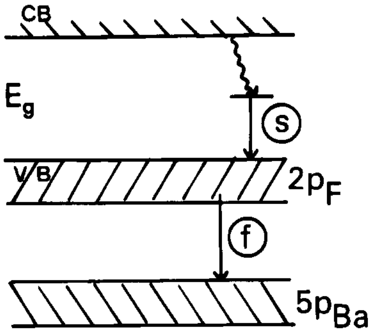

Figure 3. Emission transitions in BaF_2. s indicates the (slow) exciton recombination, and f the (fast) cross luminescence. CB indicates the conduction band, VB the valence band, and $5p_{Ba}$ the core band.

exciton recombination (see also below). Excitation with energies above 18 eV yields, in addition, another emission, which is situated around 200 nm and shows a very short decay time, viz. 0.6 ns.[18] The higher energy excitation produces cation excitons which recombine in an unexpected way: an electron jumps from the F^- ion (2p oribital) into the hole in the 5p orbital of Ba^{2+} (see Figure 3). This is accompanied by emission at 220 nm, and weaker emissions at even shorter wavelengths. It is essential that the energy difference between the 2p (F^-) and the 5p (Ba^{2+}) energy bands is less than the bandgap energy, since otherwise this so-called cross luminescence cannot be emitted. The 200-nm emission shows little temperature quenching up to room temperature, whereas the 300-nm emission is for the greater part quenched at room temperature.

Since BaF_2 is not hygroscopic, large crystals can be grown, and its density is 4.88 g cm^{-3}, the fast component shows promising potential for applications. Unfortunately its light yield is low, viz. some 1500 photons/MeV. The partially quenched slow emission has a light yield which is about a factor of 7 higher.[4] After correction for the quenching, the total energy efficiency at room temperature is estimated to be about 10%; unfortunately, the fast component contributes only one tenth to this value. The reason for this is not clear.

The BaF_2 scintillator can also be used for particle discrimination (see section 3). The intensity ratio of the fast and the slow components of the emission depends again on the nature of the excitation: the heavier the exciting particles are, the less fast emission there is. The literature does not contain an explanation for this effect. However, a reasoning parallel to that given for organic scintillators seems to be obvious. Heavy particles will not penetrate deeply into the scintillator, so that the excitation density along their track is high. At room temperature the exciton in BaF_2 will be more mobile than the electron–hole pair responsible for the cross luminescence. Therefore Auger interactions will affect the fast component more strongly than the slow component, since the hole in the 5p(Ba^{2+}) core band cannot be mobile.

At the moment there is excellent agreement between the observed emission spectrum of the cross luminescence of BaF_2 and the spectrum obtained from an ab initio calculation on basis of a molecular cluster approach.[19] This confirms the spectral assignment. These topics have been reviewed at several places.[4,20]

Table 3. On the Possibility of Cross-Luminescence[4]

compound	$E_c - E_{VB}$[a] (eV)	E_g[b] (eV)	predicted[c]	obsd[d]
BaF_2	4.4–7.8	10.5	+	+
SrF_2	8.4–12.8	11.1	0	–/STE
CaF_2	12.5–17.3	12.6	–	–/STE
CsCl	1–5	8.3	+	+
CsBr	4–6	7.3	+	+
CsI	0–7	6.2	0	–/STE
KF	7.5–10.5	10.7	+	+
KCl	10–13	8.4	–	–/STE

[a] Energy difference between top of core band and bottom or top of the valence band. [b] Energy gap. [c] +: cross luminescence (CL) possible. –: CL impossible. 0: CL doubtful. [d] +: CL observed. –: no CL observed. STE: exciton emission observed.

Table 4. Scintillators with Cross-Luminescence at 300 K[4]

compound	emission max (nm)	light yield (photons MeV^{-1})	τ (ns)
BaF_2	195, 220	1400	0.8
CsF	390	1400	2.9
CsCl	240, 270	900	0.9
RbF	203, 234	1700	1.3
$KMgF_3$	140–190	1400	1.5
$KCaF_3$	140–190	1400	<2
KYF_4	140–190	1000	1.9
$LiBaF_3$	230	1400	1
$CsCaCl_3$	250, 305	1400	<1

In view of the strong interest in very fast scintillator emission, it is not surprising that many other compounds have been investigated for cross-luminescence. It is of course essential, that the cross-luminescence emission energy is smaller than the bandgap energy, since otherwise the cross-luminescence cannot be emitted (see also Figure 3). This is illustrated in Table 3.[4] The table shows excellent agreement between prediction and observation.

Table 4, finally, shows some compounds for which cross luminescence has been definitely observed.[4] All decay times are of the same order of magnitude (~1 ns), whereas the light yields do not surpass the level of 2000 photons MeV^{-1}. It is, at this time, too early to predict whether cross luminescence will have an important application or not.

Recently, it has been shown[21,22] that dopants can also induce this type of cross luminescence, for example, Cs^+ in KCl, $SrCl_2$, and $RbCaCl_3$. This emission originates from a $CsCl_n$ cluster, and can be formulated as a radiative transition from 3p (Cl^-) and 5p (Cs^+) states.

4.4. Scintillators Based on Alkali Metal Halides. The emission of the alkali metal halides is known for a long time. Its nature was unravelled in the 1960s when it was shown that this emission is due to the following type of anion exciton recombination: The exciton exists of a hole which binds two X^- (halide) ions forming an X_2^- pseudomolecule, also called a V_K center, and an electron circling around the V_K center. The emission appears when the electron recombines with the hole. Recently it has been shown that the X_2^- pseudomolecule can move to the lattice site of one X^- ion (this is called

---

(18) Valbis, Ya. A.; Rachko, Z. A.; Yansons, Ya. L. *JETP Lett.* **1985**, *42*, 172; Aleksandrov, Yu. M.; Makhov, V. N.; Rodnyi, P. A.; Syreinshchikova, T. I.; Yakimenko, M. N. *Sov. Phys. Solid State* **1984**, *26*, 1734.

(19) Andriessen, J.; Dorenbos, P.; van Eijk, C. W. E. *Mol. Phys.* **1991**, *74*, 535; *Nucl. Tracks Radiat. Meas.* **1993**, *21*, 139.

(20) Rodnyi, P. A. *Sov. Phys. Solid State* **1992**, *34*, 1053.

(21) Voloshinovskii, A. S.; Mikhailik, V. B.; Syrotyuk, S. V.; Rodnyi, P. A. *Phys. Status. Solidi b* **1992**, *173*, 739.

(22) Sobolev, A. B. *Phys. Solid State* **1993**, *35*, 1111.

Table 5. Some Properties of Scintillators Based on Alkali Metal Halides[4,25,26]

property	NaI:Tl$^+$	CsI:Tl$^+$	CsI:Na	CsI
density (g cm^{-3})	3.67	4.51	4.51	4.51
emission max (nm)	415	560	420	315
light yield (photons MeV^{-1})	40.000	55.000	42.000	2.000
decay time (ns)	230	1000	630	16
afterglow (% after 6 ms)	0.3–5	0.5–5	0.5–5	
stability	hygroscopic	hygroscopic	hygroscopic	hygroscopic
mechanical behavior	brittle	deformable	deformable	deformable

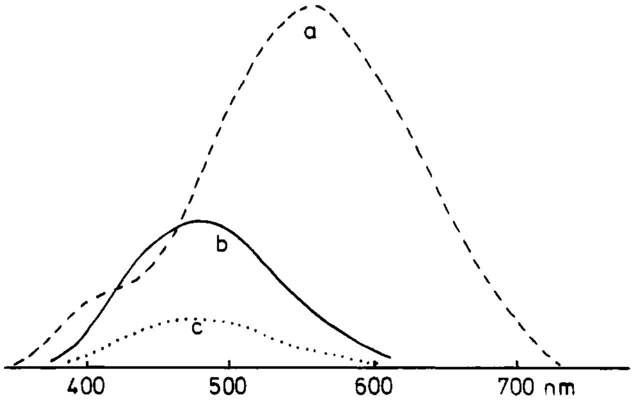

Figure 4. X-ray excited emission spectra of various scintillators. (a) CsI:Tl. (b) $ZnWO_4$. (c) $Bi_4Ge_3O_{12}$.

an H center) and the electron to the other, now vacant X^- site (forming the well-known F center). This new relaxed-excited state is an F·H pair. After emission, the F·H configuration relaxes back to the ground state, i.e., $e_X\cdot(X_2^-)_X \rightarrow 2X_X^-$. For full details the reader is referred to the literature.[23,24] If the temperature is high enough, this exciton state becomes mobile and migrates through the halide lattice.

Table 5 presents the properties of the alkali metal halides used as scintillators.[4,25,26] Pure CsI shows emission due to anion exciton recombination. Its yield is low, since this emission is for the greater part quenched at room temperature. As a consequence, the decay time is very short, since the nonradiative transitions shorten the life time of the excited state. This is attractive for applications which require a short life time without a high light yield.

In CsI:Na the emission is due to the same exciton but now bound to the sodium ion. The more widely used alkali metal halide scintillators are those activated with Tl$^+$ ($6s^2$). In these materials the migrating exciton is trapped by Tl$^+$ from where the emission occurs (see Figure 4). The transition is an interconfigurational 6s6p → $6s^2$ transition ($^3P_1 \rightarrow {}^1S_0$).

Clearly these scintillators are not of use for every application: their stability is poor, the decay time is long, and the afterglow is considerable. It is usually assumed that this afterglow is due to hole trapping in the host lattice, i.e., the V_K center is trapped somewhere, whereas the electron is trapped by the activator forming Tl°. In this way electron–hole recombination is considerably delayed, so that the emission appears much later than expected from the lifetime of the excited state of the activator.

A clear example of an application in which afterglow is unacceptable is computed tomography (CT, see above). The detector has to produce many pictures after eachother in a short time. If there is a considerable amount of afterglow, information of the first shot overlaps that of the second. Modern CT scanners require afterglow levels of <0.1% a few milliseconds after termination of the excitation pulse. From table V it is clear that the alkali metal halides cannot satisfy such a requirement.

Belsky et al.[27] have recently described evidence for a new luminescence mechanism in CsI. Apart from the exciton emission described above, there is a fast intrinsic luminescence (FIL) which can only be excited with energies ≥20 eV. It is assumed that the luminescent centers are created as the result of a strong interaction between hot excitations.

Recently, doped alkali metal halides have been suggested as efficient storage phosphors: KBr:In[28] and KBr:Eu.[29] Electrons are stored as F centers, and holes close to the dopant. Stimulation starts with ionization of the F center.

4.5. $Bi_4Ge_3O_{12}$ (BGO).

The compound $Bi_4Ge_3O_{12}$ is an interesting scintillator, from a theoretical as well as from a practical point of view. It is applied in positron emission tomography (PET) scanners and in high-energy-physics calorimeters,[1] and its crystal growth has been refined to a high degree of perfection.[30]

$Bi_4Ge_3O_{12}$ crystallizes in the cubic eulytite structure. This structure consists of isolated GeO_4 tetrahedra and Bi^{3+} ions which have their well-known asymmetric coordination: three Bi–O distances of 2.16 Å on one side of the ion and three of 2.60 Å on the other.[31] This asymmetrical coordination determines the luminescence properties.[32] In the excited state the coordination is more symmetrical. Therefore the emission transition occurs between two strongly shifted parabolas in the configurational coordinate diagram, so that a broad band appears in the spectrum (see Figure 4). As a consequence the excited state is highly localized, so that no energy migration occurs.

However, the large parabola shift, evidenced by a huge Stokes shift of the emission, implies a drawback, namely, a low thermal quenching temperature of the emission.[32] At room temperature about two-thirds of the low-temperature light yield is quenched. The theoretical energy efficiency of $Bi_4Ge_3O_{12}$ is estimated

---

(23) Song, K. S.; Baetzold, R. C. In *Defects in Insulating Materials*; Kanert, O., Spaeth, J. M., Ed.; World Scientific: Singapore, 1993; p 69.

(24) Tanimura, K.; Makimura, T.; Shibata, T.; Itoh, N.; Tokizaki, T.; Iwai, S.; Nakamura, A., p 84 in ref 23.

(25) *Scintillator Detectors*; Harshaw QS: Saint-Gobain, Nemours, 1992.

(26) Rossner, W.; Grabmaier, B. C. *J. Lumin.* **1991**, *48/49*, 29.

(27) Belsky, A. N.; Vasilėv, A. N.; Mikhailin, V. V.; Gektin, A. V.; Martin, P.; Pedrini, C.; Bouttet, D., *Phys. Rev. B*, in press.

(28) Trinkler, L. E.; Trinkler, M. F.; Popov, A. I. *Phys. Status Solidi b* **1993**, *180*, K31.

(29) Nanto, H.; Murayama, K.; Endo, F.; Hirai, Y.; Taniguchi, S.; Takeuchi, N. *J. Lumin.*, in press.

(30) Chongfau, H. Cited by Gevay, G. *Progr. Cryst. Growth Charact.* **1987**, *15*, 181.

(31) Durif, A.; Averbuch-Pouchot, M. *C.R. Ac. Sci. Paris II* **1982**, *295*, 555.

(32) Blasse, G. *Prog. Solid State Chem.* **1988**, *18*, 79.

Table 6. Some Properties of $Bi_4Ge_3O_{12}$ and of the Tungstate Scintillators[4,25,26]

property	$Bi_4Ge_3O_{12}$	$ZnWO_4$	$CdWO_4$
density (g cm^{-3})	7.13	7.87	7.99
emission max (nm)	480	480	480
light yield (photons MeV^{-1})	9.000	10.000	14.000
decay time (ns)	300	5000	5000
afterglow (% after 3 ms)	0.005	<0.1	<0.1
stability	good	good	good
mechanical behavior	brittle	brittle	brittle

to be 6% (see section 2). The experimental value at room temperature is 2%, which equals one-third of the estimated value, in agreement with the amount of thermal quenching.[2] In Table 6 some scintillator properties of BGO are presented.[4,25,26] Its strong points are high density, good stability, and weak afterglow. However, the light yield is not very high, nor is the decay time very short.

4.6. Tungstates. Tungstates have a long history in this field, since $CaWO_4$ was the very first X-ray phosphor, introduced in 1896, 1 year after Röntgen's large discovery.[33] The emission transition in the tungstate group is due to a charge-transfer transition between tungsten and oxygen.[2] As in $Bi_4Ge_3O_{12}$, the excited state is strongly distorted from the ground state, so that the emission is of the broad-band type with a large Stokes shift. In a few tungstates the amount of quenching at room temperature can be neglected and quantum efficiencies of about 70% can be obtained.

In view of their high densities, the compounds $ZnWO_4$ and $CdWO_4$, both of wolframite structure, have attracted the interest of the scintillator world. Some relevant data are given in Table 6 and Figure 4.[4,25,26] Their light yields are moderate. The reason for this can be found by performing the estimation described in section 2. As an example we consider $CdWO_4$. From the light yield and emission wavelength, the experimental value of η is 3.5%. For X-ray excitation of $CaWO_4$ powders 5% has been reported.[33] With $\beta = 7$, $E_g = 5$ eV, $S = 1$ and $q = 0.7$, the estimated value is 6%. From this we learn that η will be low anyhow (mainly due to the high value of β) and that higher values than 3.5% are not very realistic, since S will be certainly smaller than 1.

Further, the afterglow is weak, but the decay time long. Although tungstate crystals are usually stable in the atmosphere, they cleave easily which makes machining difficult.[26] Finally, $CdWO_4$ is toxic.

Photoluminescence specialists may be surprised to see nowadays compounds like $NaBi(WO_4)_2$ and $PbWO_4$ presented as new scintillators, because under ultraviolet excitation these compounds hardly luminesce at room temperature. $PbWO_4$[1,34] and $NaBi(WO_4)_2$[1] have scheelite structure (like $CaWO_4$) with very high densities (8.2 and 7.6 g cm^{-3}, respectively). Their light yields are indeed very low: ~100 photons/MeV (i.e., $\eta \sim 0.025\%$). The decay times are very short, a few nanoseconds. This value is mainly determined by the nonradiative transition rate, since the luminescence is practically quenched. These materials may be of interest for those who want fast decay and high density without any requirements to the light yield (high-energy physics calorimeters).

Table 7. Some Properties of Ce^{3+}-Activated Scintillators[1,4,25,40,52]

host lattice	Ce^{3+} concn (mol %)	emission max (nm)	light yield (photons MeV^{-1})	decay time (ns)	density (g cm^{-3})
BaF_2	0.2	310, 325	7000	60[a]	4.89
LaF_3	10	290, 305	900	27	5.89
CeF_3	100	310, 340	4000	40	6.16
$YAlO_3$	0.1	350, 380	17000	30	5.55
Gd_2SiO_5	0.5	440	9000	60[a]	6.71
Lu_2SiO_5		420	25000	40	7.4
glass[b]	4	390	1500	70[a]	2.5
$Y_3Al_5O_{12}$	0.4	550	14000	65	5

[a] And longer component. [b] Composition $(SiO_2)_{0.55}(MgO)_{0.24}(Al_2O_3)_{0.06}(Li_2O)_{0.06}(Ce_2O_3)_{0.04}$.

4.7. Ce^{3+}-Doped Silicates. Compounds with stoichiometry Ln_2SiO_5 (Ln = lanthanide) have been reported to be efficient luminescent materials for decades. In 1969 $Y_2SiO_5{:}Ce^{3+}$ was proposed as a cathode-ray phosphor in flying-spot scanners[35] and $Y_2SiO_5{:}Tb^{3+}$ as a green cathode-ray phosphor.[36,37] Later, $Gd_2SiO_5{:}Tb^{3+}$ was proposed as an X-ray phosphor.[38] Recently it has been reported that $Gd_2SiO_5{:}Ce^{3+}$ and $Lu_2SiO_5{:}Ce^{3+}$ are efficient scintillators.[39,40] In the mean time the crystal structures have been determined by Felsche.[41] Using the Czochralski method, crystals can be grown approximately 20 mm in diameter and 50 mm in length.[42] Some properties of interest are given in Table 7.

Gd_2SiO_5 has a complicated crystal structure with two different crystallographic sites for the lanthanide ions. It is not hygroscopic, but it cleaves easily, which can be a problem for certain applications. To a limit degree $Gd_2SiO_5{:}Ce^{3+}$ is applied in positron emission tomography and oil-well logging.

The luminescence of Ce^{3+} ($4f^1$) consists of a 5d → 4f transition. It is a band emission with a double maximum due to the splitting of the ground state configuration ($4f^1 \rightarrow {}^2F_{7/2}$ and ${}^2F_{5/2}$). This transition is an allowed one, so that the decay time τ is short (see Table 7). For many applications this is an interesting fact. Since the emission of Ce^{3+} in these silicates peaks in the blue, the value of τ is relatively long (~50 ns), since $\tau \sim \lambda^2$, where λ gives the emission wavelength. The light yield of $Gd_2SiO_5{:}Ce^{3+}$, although not low, is below what can be expected (η_{obs} ~2.5%, η_{est} ~8%).

Suzuki et al.[39] have reported on the ultraviolet and γ-ray excited luminescence of $Gd_2SiO_5{:}Ce^{3+}$. At 11 K they were able to find luminescence from two different Ce^{3+} ions, one with an emission maximum at about 425 nm, the other with an emission maximum at about 500 nm (see Figure 5). The respective lowest excitation bands have their maxima at 345 and 380 nm, and their respective decay times are 27 and 43 ns. The former luminescence is hardly quenched at room temperature, the intensity of the latter decreases above 200 K, and at room temperature only 20% remains. Under γ-ray

---

(33) Brixner, L. H. *Mater. Chem. Phys.* **1987**, *16*, 253.

(34) Kobayashi, M.; Ishii, M.; Usuki, Y.; Yahagi, H. *Nucl. Instrum. Methods* **1993**, *A333*, 429.

(35) Gomes de Mesquita, A. H.; Bril, A. *Mater. Res. Bull.* **1969**, *4*, 643; *J. Electrochem. Soc.* **1969**, *116*, 871.

(36) Peters, T. E. *J. Electrochem. Soc.* **1969**, *116*, 985.

(37) Ronda, C. R.; Kynast, U. H.; Dingen, W. P. M.; van Hal, H. A. M. *J. Alloys Comp.* **1993**, *192*, 55.

(38) Lammers, M. J. J.; Blasse, G. *J. Electrochem. Soc.* **1987**, *134*, 2068.

(39) Suzuki, H.; Tombrello, T. A.; Melcher, C. L.; Schweitzer, J. S. *Nucl. Instrum. Methods* **1992**, *A320*, 263.

(40) Melcher, C. L.; Schweitzer, J. S. *Nucl. Instrum. Methods* **1992**, *A314*, 212.

(41) Felsche, J. *Struct. Bonding* **1973**, *13*, 99.

(42) Melcher, C. L.; Manente, R. A.; Peterson, C. A.; Schweitzer, J. S. *J. Cryst. Growth* **1993**, *128*, 1001.

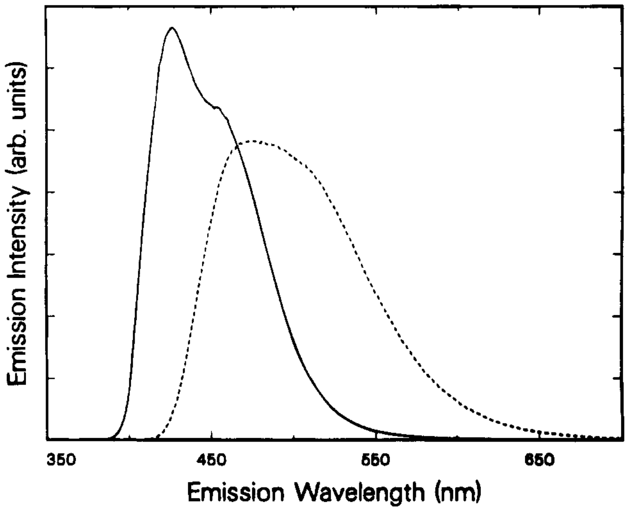

Figure 5. The two Ce^{3+} emission bands of $Gd_2SiO_5:Ce^{3+}$ at 11 K. After ref 39.

excitation at room temperature the luminescence is dominated by the 425-nm emission, since the other is quenched for the greater part. Peculiarly enough, the decay shows under these conditions, a long component ($\tau \sim 600$ ns), which is not observed for $Y_2SiO_5:Ce^{3+}$ nor $Lu_2SiO_5:Ce^{3+}$.

It is possible to propose a simple explanation for these experimental observations. First we note that the ratio of the decay times ($\sim 0.6^5$) is about equal to the squared ratio of the emission band maxima ($\sim 0.7^5$) as is to be expected from the $\tau \sim \lambda^2$ relation.

The long decay component of $Gd_2SiO_5:Ce^{3+}$ can be ascribed to the fact that part of the electron–hole pairs formed by γ-ray irradiation are captured by Gd^{3+} ions. The excitation energy migrates over the Gd^{3+} ions as described in refs 14 and 32. In this way the Ce^{3+} ions are populated in a delayed manner, so that a long decay component is observed. This effect does not occur in $Y_2SiO_5:Ce^{3+}$ nor in $Lu_2SiO_5:Ce^{3+}$, since the host lattice ions do not have energy levels below the bandgap energy.

The crystal structure of Gd_2SiO_5 shows that one Ce^{3+} ion is coordinated by eight oxygen ions belonging to silicate tetrahedra and one oxygen which is not bonded to silicon. The latter oxygen is coordinated tetrahedrally by four rare earth ions. The other Ce^{3+} ion is coordinated by four oxygen ions belonging to silicate tetrahedra and three oxygen ions which are not. The latter Ce^{3+} ion is more strongly covalently bonded, because the oxygen ions without silicon neighbors do not have enough positive charge in their immediate surroundings to compensate their twofold negative charge.[38] Consequently, this Ce^{3+} ion has its energy levels at lower energy, as has also been observed for Tb^{3+} in Gd_2SiO_5.[38]

Finally the lower quenching temperature of this Ce^{3+} emission remains to be explained. It is important to note that the oxygen ions, coordinated by four rare-earth ions only, form a two-dimensional network in the crystal structure of Gd_2SiO_5. The longer wavelength emitting Ce^{3+} ions are located in this network. There is a striking structural analogy with the structure of Y_2O_3 where every oxygen is tetrahedrally coordinated by four yttrium ions, so that the network is three dimensional. Actually Ce^{3+} in Y_2O_3 does not luminesce due to photoionization.[43] In $Ca_4GdO(BO_3)_3$ the Ce^{3+} ion also does not luminesce.[44] In this host lattice a similar structural network can be distinguished. Therefore we conclude that the low quenching temperature of the Ce^{3+} ion in Gd_2SiO_5 which is coordinated by three oxygen ions, which do not coordinate to silicon, must be explained in the same way.

The quenching of one of the two Ce^{3+} centers in Gd_2SiO_5 is at least partly responsible for the discrepancy between the observed and theoretical values of the efficiency.

The host lattice Lu_2SiO_5 has a different crystal structure which is also the structure of Y_2SiO_5. Luminescence studies do not show a large amount of quenching of the Ce^{3+} emission at room temperature.[39] It is therefore not surprising that in this structure much higher light yields can be obtained than in Gd_2SiO_5. The experimental values are close to the theoretical maximum (see Table 7). It has been found that $Y_2SiO_5:Tb^{3+}$ yields under X-ray excitation also a higher efficiency than $Gd_2SiO_5:Tb^{3+}$.[38] This suggests that the Gd_2SiO_5 structure contains in some way centers which compete with the activator ions for the capture of charge carriers. The scintillator $Lu_2SiO_5:Ce^{3+}$ seems, therefore, to have many advantages. Unfortunately, the cost of pure Lu_2O_3 is extremely high.

4.8. CeF_3. Some properties of CeF_3 as a scintillator are included in Table 7. This material is a serious candidate for a new generation of high-precision electromagnetic calorimeters to be used for the new large proton collider to be built at CERN (Geneva). For that purpose one needs a total crystal volume as large as 60 m^3,[11] which is nearly 2 orders of magnitude more than at present (1.2 m^3 $Bi_4Ge_3O_{12}$). As mentioned, the relatively low light yield of CeF_3 is not detrimental for this specific application. In view if these plans a large amount of research has already been performed on CeF_3.[45–47] In passing it should be mentioned that the high costs of this proposal have forced the scientists involved to look for a cheaper solution based on a reasonable compromise between cost and performance.

The spectroscopy of the Ce^{3+} ion is relatively simple due to its one-electron configuration $4f^1$.[48] The compound CeF_3 is a material with 100% activator concentration. As in the case of $Bi_4Ge_3O_{12}$ (see also ref 32), the relatively large Stokes shift of the emission localizes the excited state, so that concentration quenching by energy migration to quenching sites does not occur. Actually, CeF_3 was already known in the early 1940s to be an efficient photoluminescent material.[49]

The paper by Moses et al.[45] on the scintillation properties of CeF_3 is a fine example of how scintillators should be studied from a fundamental point of view. A combination of techniques was used, including (time-resolved) luminescence spectroscopy, ultraviolet photoelectron spectroscopy, transmission spectroscopy, and

---

(43) Blasse, G.; Schipper, W. J.; Hamelink, J. J. *Inorg. Chim. Acta* **1991**, *189*, 77.

(44) Dirksen, G. J.; Blasse, G. *J. Alloys Comp.* **1993**, *191*, 121.

(45) Moses, W. W.; Derenzo, S. E.; Weber, M. J.; Cerrina, F.; Ray-Chaudhuri, A. *J. Lumin.* **1994**, *59*, 89.

(46) Pedrini, C.; Moine, B.; Boutet, D.; Belsky, A. N.; Mikkhailin, V. V.; Viselev, A. N.; Zinin, E. I. *Chem. Phys. Lett.* **1993**, *206*, 470.

(47) Crystal Clear Group; Lecoq, P., secretary general; *Nucl. Instrum. Methods* **1993**, *A332*, 373.

(48) Weber, M. J., p 99 in ref 1.

(49) Kröger, F. A.; Bakker, J. *Physica* **1941**, *8*, 628.

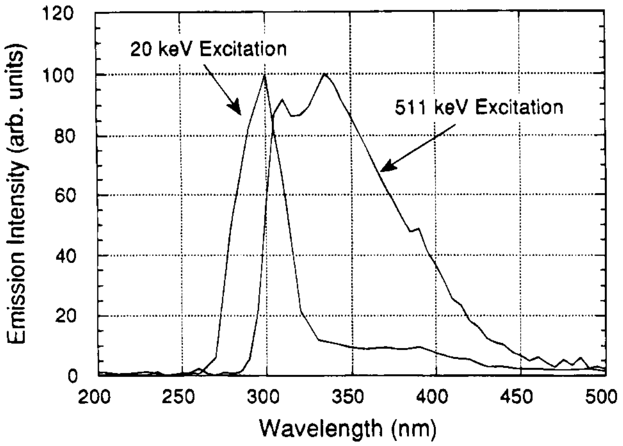

Figure 6. Emission spectra of powdered CeF$_3$ (20-keV X-ray excitation) and crystalline CeF$_3$ (511 keV γ-rays). After ref 45.

the excitation region was extended up to tens of electronvolts by using synchrotron radiation. Further, powders as well as crystals with composition La$_{1-x}$Ce$_x$F$_3$ were investigated.

The emission depends strongly on the value of x and on the excitation energy (see also Figure 6). The intrinsic Ce^{3+} emission consists of a narrow band with maxima at 284 and 300 nm. These are ascribed to transitions from the lowest level of the 5d configuration to the two levels of the 4f ground configuration ($^2F_{5/2}$, $^2F_{7/2}$). If $x > 0.1$, an additional emission band appears at longer wavelength (around 340 nm) which sometimes even dominates (see Figure 6). This one is ascribed to Ce^{3+} ions close to defects.

Instructive is the emission for $x \leq 0.01$: it consists of the intrinsic Ce^{3+} emission band, Pr^{3+} emission lines, and broad band extending from 250 to 500 nm which is ascribed to self-trapped exciton (STE) emission from the host. The STE consists of an electron bound to a V$_K$ center which is a hole trapped by two fluorine ions forming a pseudomolecule F$_2^-$. This shows that the lattice itself also traps the electron–hole pairs. At room temperature the STE migrates over the lattice, ending its life by radiative recombination, transfer to Ce^{3+} or to Pr^{3+} (the latter being present as an impurity), or by nonradiative recombination. This illustrates that for this composition the factor S in eq 1 is far from one if one considers the Ce^{3+} emission.

In CeF$_3$ energy transfer from intrinsic to extrinsic Ce^{3+} ions takes place.[45,46] Extrinsic Ce^{3+} ions are Ce^{3+} ions close to imperfections in the crystal lattice. Radiative as well as nonradiative transfer contributes. Actually the 340 nm emission shows a buildup which is equal to the decay of the 290-nm emission. The decay times of these emissions are about 30 and 20 ns, respectively. This agrees well with the $\tau \sim \lambda^2$ relation.

Under high-energy excitation, an initial much faster decay has been observed. This phenomenon was studied by Pédrini et al.[46] This fast component is of more importance if there are more defects (impurities) in the lattice. However, even in very pure crystals it is present. When a high-energy particle is absorbed, the region of its relaxation has a radius of 10–100 nm. Therefore the electronic excitation is correlated in space and time. Auger relaxation in excited pairs has been proposed as a loss mechanism. The importance of this process decreases with temperature, since the excited states become more and more mobile at higher energies, so that a pair of excited ions can dissociate.

With 4000 photons MeV^{-1} the light yield of CeF$_3$ is low. This corresponds to $\eta \sim 1\%$, whereas $\eta_{\max} \sim 8\%$. This shows that the greater part of the emission is quenched. It is usually admitted that impurity rare earth ions cannot be responsible for such a loss. However, fluoride crystals will always contain a certain (low) amount of oxygen. If the presence of O^{2-} would force one of the neighboring cerium ions to become Ce^{4+} for charge compensation, a bulky quenching center is created, since intervalence charge-transfer transitions are at low energy and yield seldom emission.[50] If we add to this loss the Auger process mentioned above, it is understandable that the light yield of CeF$_3$ is considerably lower than is to be expected.

Moses et al.[45] have determined the quantum efficiency of the CeF$_3$ luminescence. For direct Ce^{3+} excitation it is high. Lower quantum efficiencies are found if the excitation starts at the F$^-$ ion (2p). For 100 eV the total quantum efficiency is about 0.7. The energy efficiency is then 3%. This is relatively low, and the authors suggest nonradiative recombination on quenching centers in order to explain this.

4.9. Other Ce^{3+} Scintillator Materials. The strong potential of scintillators like Gd$_2$SiO$_5$:Ce^{3+}, Lu$_2$SiO$_5$:Ce^{3+}, and CeF$_3$ have prompted a search for other Ce^{3+}-activated scintillators. Recently many new ones have been proposed.[1,3,4,51,52] Some of these have been included in Table 7. New ones are still appearing.

Here we mention BaF$_2$:Ce^{3+}, YAlO$_3$:Ce^{3+}, and Y$_3$Al$_5$O$_{12}$:Ce^{3+} as potential candidates for application (see Table 7). Cerium-activated glasses which can show high photoluminescence efficiency[53] cannot be considered as efficient scintillators. Possible reasons for this were discussed above. Further there are reports on CeP$_5$O$_{14}$ ($\tau \sim 30$ ns, light yield 4000 photons/MeV,[3] LuPO$_4$:Ce^{3+} (25 ns, 17 200 photons MeV^{-1}),[3,51] CsGd$_2$F$_7$:Ce^{3+} (30 ns, 10 000 photons MeV^{-1}),[52] and GdAlO$_3$:Ce^{3+} (8000 photons MeV^{-1}).[52,54]

A slightly different approach is the use of Nd^{3+} as suggested by Van Eijk's group.[4,52] The Nd^{3+} ion has 4f^3 configuration with a 5d → 4f emission transition in the ultraviolet (~175 nm). Since this is an allowed transition at very high energy, the radiative decay time of 6 ns (in LaF$_3$:Nd^{3+}) is even shorter than for Ce^{3+}. The light yield is a few hundred photons/MeV. Several other host lattices have been tried, but light yields never surpass 1000 photons MeV^{-1}. An important problem is generated by the absorption of Nd^{3+} emission by rare-earth impurities.

4.10. Other Rare-Earth-Doped Materials. Up to this section the luminescence of rare earth ions was used because of its fast decay time (Ce^{3+}, Nd^{3+}, with an allowed 5d → 4f transition). Usually rare-earth-ion luminescence is characterized by much slower decay times (intraconfigurational 4f^n transitions, parity forbidden). This is less suitable for applications which

---

(50) Blasse, G. *Struct. Bonding* **1991**, *76*, 153.

(51) Lempicki, A.; Berman, E.; Wojtowicz, A. J.; Balcerzyk, M.; Boatner, L. A. *IEEE Trans. Nucl. Sci.* **1993**, *40*, 384.

(52) Visser, R. Thesis, Technical University Delft, 1993.

(53) Verwey, J. W. M.; Blasse, G. *Mater. Chem. Phys.* **1990**, *25*, 91; *Chem. Mater.* **1990**, *2*, 458.

(54) Mares, J. A.; Pedrini, C.; Moine, B.; Blazek, K.; Kvapil, J. *Chem. Phys. Lett.* **1993**, *206*, 9.

Table 8. Some Data of X-ray Scintillators for Computed Tomography (after Ref 26)

scintillator	CsI:Tl	$CdWO_4$	$Bi_4Ge_3O_{12}$	$(Y,Gd)_2O_3$:Eu	Gd_2O_2S:Pr,Ce,F
type	single crystal	single crystal	single crystal	ceramic	ceramic
density (g cm^{-3})	4.52	7.99	7.13	5.9	7.34
emission max (nm)	550	480	480	610	520
relative light output	100	30	10	~40	~60
decay time (μs)	1	5	0.3	~1000	~3
afterglow (%)	1 after 20 ms	0.2 after 20 ms	<0.1 after 20 ms	~5^a after 3 ms	<0.1 after 3 ms
optical quality	clear	clear	clear	transparent	translucent

^{a} After ref 56.

require fast decay times, but nevertheless the slow emission has also found a broad application.

In X-ray imaging, phosphors such as $Gd_2O_2S:Tb^{3+}$ and $LaOBr:Tm^{3+}$ are used. They were reviewed before.[14,55] In digital radiography a much faster decay (~1 μs) is required. Here $BaFBr:Eu^{2+}$ with a 5d → 4f emission transition is the most important candidate, as reviewed in ref 14.

Interesting developments are happening in the field of computed tomography, where classic scintillators are now replaced by ceramic plates consisting of rare-earth-activated material.[26,56] Table 8 gives a summary of the developments.[26] Crystals of $CsI:Tl^+$ have been widely used, although their afterglow level is high. It is generally assumed that the electron can be trapped on the activator ion, and the hole is trapped as a V_K center bound to a defect. A V_K center is a pseudomolecular I_2^- species on the site of two I^- ions in the lattice. In the case of $CdWO_4$ and $Bi_4Ge_3O_{12}$, the afterglow level is considerably less, but unfortunately the light yield is also considerably less.

Ceramic materials show also a considerable amount of afterglow after X-ray irradiation. However, by suitable codoping this can be suppressed. Considerations about codoping with a predictive power have been given in the literature.[57,58] Let us illustrate this on another ceramic material proposed as a scintillator for computed tomography, namely $Gd_3Ga_5O_{12}:Cr$.[59] This material shows a considerable amount of afterglow which can be suppressed by codoping with cerium. The afterglow can be explained by the fact that part of the electrons created by X-ray irradiation are trapped by oxygen vacancies, whereas the holes are trapped by the Cr^{3+} ions. The electrons recombine with these holes after thermal detrapping. This yields delayed luminescence.

The cerium dopant is, according to spectral measurements, in the tetravalent state. The oxygen vacancy concentration is lowered, and the Ce^{4+} ions act as a deep electron trap from where escape is difficult. In this way the afterglow is reduced, but the light yield decreases also. It will be clear that the processing of luminescent ceramic plates for possible use in computed tomography requires the utmost care and full mastering of all process conditions. The present results look very promising. Figure 7 shows the emission spectra of some ceramic materials, whereas Figure 8 illustrates the afterglow reduction upon codoping.

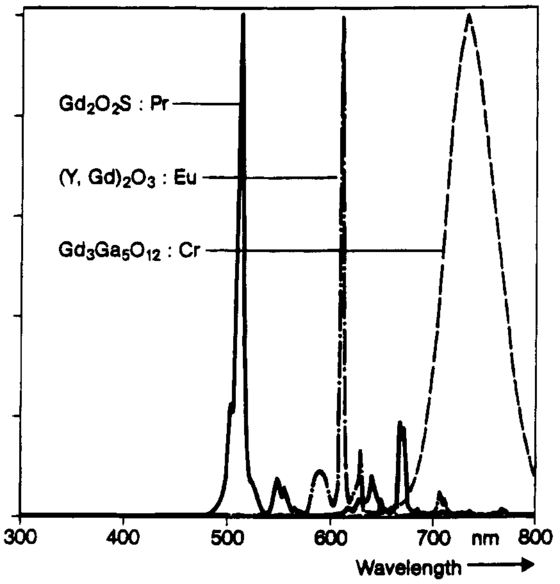

Figure 7. X-ray excited emission spectra of some ceramic scintillators. After ref 57.

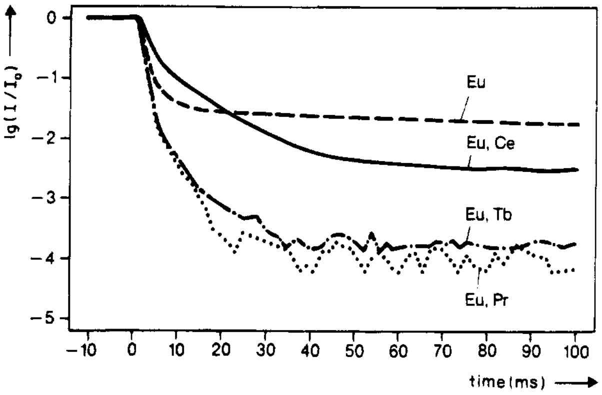

Figure 8. Afterglow behavior of $(Y,Gd)_2O_3:Eu^{3+}$ ceramics with different codopants. The end of the X-ray pulse is at $t = 0$. After ref 65.

5. The Future

Scintillator research has been performed for many years in the conviction that the physical mechanisms were unknown, that predictions were impossible, and that new materials had to be found by trial and error.[60] As shown in this review, the real situation is considerably more favorable, although many problems still remain. This section tries to survey the present situation critically and to predict future developments. For this purpose several of the scintillator properties are considered subsequently.

1. Light Yield. As argued in section 2 it is possible to estimate the factor β and, therefore, the conversion

---

(55) Brixner, L. H. *Mater. Chem. Phys.* **1987**, *16*, 253.

(56) Greskovich, C. D.; Cusano, D.; Hoffman, D.; Riedner, R. J. *Am. Ceram. Soc. Bull.* **1992**, *71*, 1120.

(57) Grabmaier, B. C. In *Defects in Insulating Materials*; Kanert, O., Spaeth, J. M., World Scientific: Singapore, 1993; p 350; *J. Lumin.* **1994**, *60/61*, 967.

(58) Blasse, G.; Grabmaier, B. C.; Ostertag, M. *J. Alloys Comp.* **1993**, *200*, 17.

(59) Tsoukala, V. G.; Greskovich, C. D. European Patent Application 0467044 A2, 24-5-91.

(60) Blasse, G. *IEEE Trans. Nucl. Sci.* **1991**, *38*, 30.

efficiency γ. These are intrinsic properties of the host lattice. Generally speaking, a lattice with low vibrational frequencies has a low value of β and a high value of γ (see also Table 1). In principle the quantum efficiency of the luminescent center can be high. According to eq 1 this leaves the transfer efficiency S as an unknown and unpredictable parameter. Host lattices with a complicated buildup will most probably have a low value of S. The value of S is not an intrinsic property, and might be optimized by varying the preparational conditions. We are able, therefore, to predict the maximum possible energy efficiency η. Whether we can realize this efficiency in practice, depends mainly on the value of S.

Two critical comments have to be made about this seemingly satisfactory situation. First, the physical processes on which the model is based have not been proven and might be different from what is expected. We may expect that synchrotron excitation experiments may help to solve this problem. In a sense they fill the wide gap between photoluminescence and X- or γ-ray excited luminescence. However, this problem has a high degree of sophistication. Second, it may seem that it is now possible to predict many new scintillator materials. However, if a high light yield is required, and if S will be low for complicated compositions, the restriction to simple host lattices implies that not many possibilities have been overlooked until now.

2. Decay Times. Short decay times (~10 ns) are found in the case of fully allowed emission transitions (for example, 5d → 4f on Ce^{3+}). Shorter decay times are hard to realize with the exception of the cross-luminescence transitions (~1 ns). Spectroscopy books (for a short review see ref 2) yield usually enough information to estimate the value of the decay time to be expected (see also ref 3). If the light yield does not play an important role, the decay time can be shortened by quenching centers or temperature quenching. An example is the case of $PbCO_3$ which has been proposed as a fast scintillator,[61] although its luminescence is quenched below 80 K.[62]

3. Afterglow. The phenomenon of afterglow is in itself understood. Guide lines to predict the way in which the afterglow level can be depressed are available in the literature.[57] However, the exact mechanism can be revealed only by studying a specific composition. Since the nature of the traps is often not known and the trap concentration is low, such a study is usually very hard to perform. This is also the reason why the physical mechanism of storage phosphors for digital radiography is still under debate and only incompletely understood.[63]

4. Emission Wavelength. Our knowledge of the energy levels of luminescent ions is nowadays at a level that the emission wavelength can be estimated with a reasonably high degree of accuracy.[2] The type of detector prescribes the emission wavelength region:[2] photodiodes 500−900 nm, photomultiplyers 200−500 nm, gas-filled detectors ≤200 nm.

5. Material Conditions. Apart from their use as powders in X-ray imaging, scintillators are mainly applied as large single crystals or ceramic plates. In both cases the preparation is cumbersome and expensive and may even restrict the selection of potential materials. The purity of the final product should always be high and its crystalline perfection superb, in order to keep the value of S high.

The preparation of glassy or organic scintillators is of course much easier, but their disadvantages are clear. Glassy materials yield a low light yield, whereas organic scintillators have a low stopping power due to their low density.

Actually, the development of a promising scintillator compound into an optimized material is a long road where, next to fundamental knowledge and chemical experience, some luck and common sense are also indispensable.

In summary, a broad knowledge of luminescent materials and luminescence phenomena is of great help in the search for and development of scintillator materials. The excitation mechanism contains still many unknown aspects which might in the future be unravelled by synchrotron excitation experiments. In this connection it is interesting to remark that commerical photoluminescent materials are also investigated in this way in order to study the possibilities of $q > 1$.[64] The afterglow mechanism differs probably from case to case and is only to be solved by using a combined number of techniques and well-characterized samples.

Acknowledgment. The author is indebted to Prof. C. W. E. van Eijk (Technical University Delft) and Prof. B. C. Grabmaier (Siemens AG, Munich, and University Utrecht) for instructive discussions on several aspects of scintillators.

---

(61) Moses, W. W.; Derenzo, S. E. *IEEE Trans. Nucl. Sci.* **1990**, *37*, 96.

(62) Lammers, M. J. J.; Blasse, G.; Brixner, L. H. *Mater. Res. Bull.* **1986**, *21*, 529.

(63) Blasse, G. *J. Alloys Comp.* **1993**, *192*, 17.

(64) Berkowitz, J. K.; Olsen, J. A. *J. Lumin.* **1991**, *50*, 111 and references therein.

(65) Grabmaier, B. C.; Rossner, W.; Leppert, J. *Phys. Status Solidi a* **1992**, *130*, K183.